Using Magnetic Levitation for Non-Destructive Quality Control of Plastic Parts

*Jonathan W. Hennek, Alex Nemiroski, Anand Bala Subramaniam, David K. Bwambok, Dian Yang, Daniel V. Harburg, Simon Tricard, Audrey K. Ellerbee, and George M. Whitesides**

Large-scale, reliable, and economical manufacturing of plastic objects ("parts")[1] is critical for a range of industrial applications (e.g., medical devices, automotive parts, small consumer goods, microelectromechanical systems (MEMS), and optical devices, among others). Plastic parts are chosen (over metal, for example) in many cases, in order to lower the cost (as well as weight, corrosion resistance, and other properties) of the final assembled product. Depending on the scale of manufacturing, costs favor relatively simple techniques such as injection molding, casting, stamping, or machining for producing products with a range of shapes from raw, polymeric plastics.[1] Low-cost plastic parts must maintain an acceptable level of quality to avoid failure in use. In an optimized production process, occasional defects, such as voids, cracks, or embedded impurities can occur during routine manufacturing.[2–7] Defective parts, if not identified, can lead to the failure of the final assembled product. Non-destructive methods are thus required to identify defective parts that deviate from quality standards resulting either from manufacturing (both process optimization and volume production) or improper storage or use of the part.

Current non-destructive methods that have been used to test the quality of molded parts in specialized and critical applications include industrial computed tomography (ICT),[8,9] infrared thermography,[10] and ultrasonic testing.[11] The cost and complexity associated with the use of these instruments often prevent their application in routine quality control and, therefore, during the development and use of a manufacturing process visual inspection may be the only form of quality control. In this paper, we demonstrate how magnetic levitation (MagLev) enables: i) the identification of parts with embedded defects, ii) the separation of a defective part from a single batch, iii) the characterization of certain kinds of defects, and iv) the detection of counterfeit, high-value plastic parts. MagLev can suspend, localize, and orient[12] an object without contact with a solid surface, such as a gripper or solid wall, by balancing gravitational and magnetic forces.[13] Here, we show that the orientation of a part that is magnetically levitated depends strongly on both its shape and heterogeneity in density. This characteristic enables rapid identification of a defective part by visual inspection of the levitation height or angle of orientation in comparison to the rest of the parts in the batch. The method is inexpensive, non-destructive, and straightforward to implement. The portability of the MagLev device has the potential to allow quality control of parts at the point-of-manufacturing, the point-of-sale, and the point-of-use.

We used a similar MagLev device setup to those previously described.[13] Briefly, the object is suspended in a container filled with a paramagnetic solution (e.g., aqueous manganese chloride, $MnCl_2$, or paramagnetic ionic liquids)[14] and the container is placed between two NdFeB magnets oriented with like poles facing each other (**Figure 1**). In this configuration of the magnets, the magnetic gradient along the vertical centerline is approximately linear, and the vertical equilibrium position of the diamagnetic object within the device—its levitation height, h, measured as the distance between the face of the bottom magnet to the centroid of the object—correlates linearly with its volume-averaged density $\overline{\rho}_s$ (kg m^{-3}), as shown in Equation 1:[13]

$$h = \frac{(\overline{\rho}_s - \rho_m) g \mu_o d^2}{(\overline{\chi}_s - \chi_m) 4 B_0^2} + \frac{d}{2} \quad (1)$$

In this equation, ρ_m (kg m^{-3}) is the density of the paramagnetic medium, $\overline{\chi}_s$ is the volume-averaged magnetic susceptibility of the sample (Supporting Information, unitless), χ_m is the magnetic susceptibility of the medium (Supporting Information, unitless), d (m) is the distance between the magnets, B_0 (T) is the magnitude of the magnetic field at the surface of the magnets, g (m s^{-2}) is the acceleration due to gravity, and μ_o (T m A^{-1}) is the magnetic permeability of free space.

We and others have used MagLev to classify forensic evidence,[15] analyze biological systems,[16,17] determine the quality of food,[18] separate crystal polymorphs,[19] separate enantiomers and racemates,[20] study fundamental particle–fluid interactions,[21]

Dr. J. W. Hennek, Dr. A. Nemiroski, Prof. A. B. Subramaniam, Dr. D. K. Bwambok, Dr. D. V. Harburg, Dr. S. Tricard, Prof. A. K. Ellerbee, Prof. G. M. Whitesides
Department of Chemistry and Chemical Biology
Harvard University
12 Oxford St., Cambridge, MA 02138, USA
E-mail: gwhitesides@gmwgroup.harvard.edu
D. Yang
School of Engineering and Applied Sciences
Harvard University
29 Oxford St., Cambridge, MA 02138, USA
Prof. G. M. Whitesides
Wyss Institute for Biologically Inspired Engineering
Harvard University
60 Oxford St., Cambridge, MA 02138, USA
Prof. G. M. Whitesides
Kavli Institute for Bionano Science and Technology
Harvard University
29 Oxford Street, Cambridge, MA 02138, USA

DOI: 10.1002/adma.201405207

ADVANCED MATERIALS
www.advmat.de

www.MaterialsViews.com

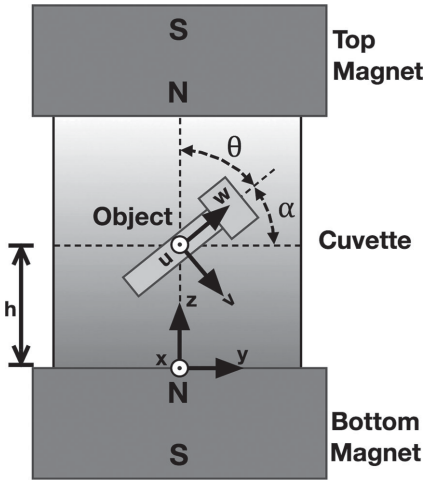

Figure 1. A schematic of the MagLev device used in this work. Plastic parts to be analyzed are placed within a container of paramagnetic medium and levitate at a height, *h*, above the surface of the bottom magnet where the gravitational and magnetic forces balance. We define the laboratory frame of reference with coordinates (*x*,*y*,*z*) and the body-fixed, principal frame of reference with coordinates (*u*,*v*,*w*). For an object with heterogeneity in density, the orientation of the object can be measured as an angle θ between the *w*- and *z*-axes or as an angle α between the *w*- and *y*-axes.

and provide an environment for self-assembly,[22] among other applications.[23–32] The range of densities that can be measured simply with MagLev (ρ between 0.8 and 3.0 g cm^{-3}) matches well with the characteristics of polymers, and thus with the needs of polymer analysis. Table S1 in the Supporting Information gives values of density for various solid polymers and other materials for which MagLev might be applied.

Recently, we used MagLev to orient and assemble objects in 3D without mechanical contact.[12] We showed that objects of homogenous density, but of anisotropic shape, oriented with their long axis parallel or perpendicular to the surface of the magnets in a manner that depended on their aspect ratio (i.e., the ratio between the width and length of an object).[12] The analytical model developed in that work suggested that objects with regions of heterogeneous density should deviate from this behavior. We thus hypothesized that observing the orientation that a part adopts in a MagLev device might be a means to detect defects in plastic parts.

To test this hypothesis, we selected a commercial batch of plastic parts consisting of 23 Nylon 6 washers purchased from McMaster–Carr. All the washers appeared undamaged and free from defects by visual inspection (although they were opaque). We levitated each of the washers sequentially in a solution of 0.10 M $MnCl_2$ + 1.26 M $ZnCl_2$ and measured α, the angle that the washer oriented with respect to the surface of the magnets. We plotted a histogram of the values of α in **Figure 2**A. Most of the washers levitated with α = 0–16°; this narrow distribution indicated that the washers were relatively homogeneous. This observation is expected since the washers were produced using an optimized process. One washer deviated significantly, however, and levitated at α = 45° (Figure 2B).

Since each of these washers appeared visually indistinguishable, we reasoned that an internal defect could have led to the observed deviation in α. We thus performed microcomputed

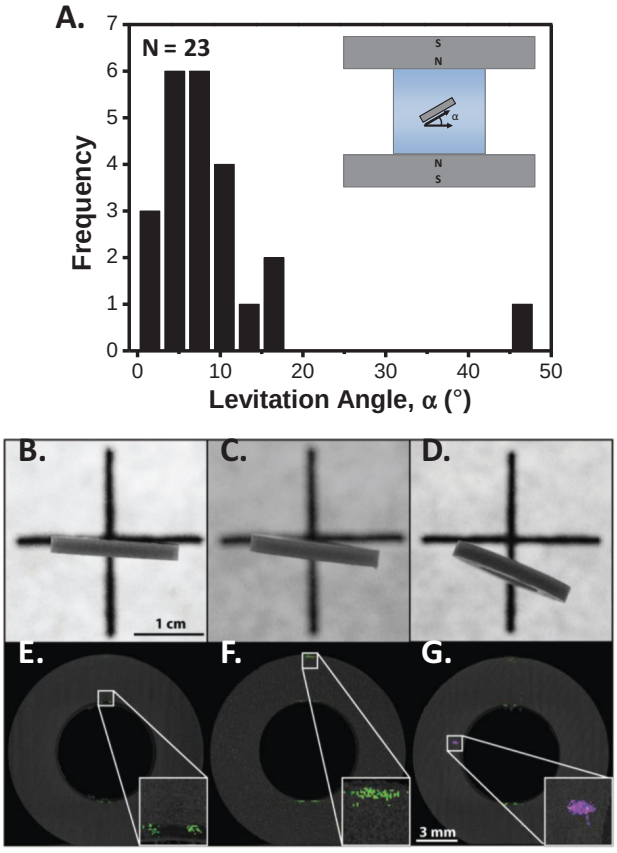

Figure 2. A) Histogram of a batch of Nylon 6 washers showing distribution in their levitation angle, α, measured horizontal to the face of the magnet, typically <16° in 0.10 M $MnCl_2$ + 1.26 M $ZnCl_2$. The angle for one washer deviated significantly (α = 45°). Photographs show three washers levitating at ≈3° B), 10° C), and 45° D). The cross in the background is a visual reference. Images have been modified to increase contrast. E–G) Micro-CT images of the same washers showing similar porosity (green) in all and an inclusion (0.014 mm^3) with a greater density in the abnormal washer, leading to a different levitation height.

tomography (micro-CT) on the washer that was an outlier (α = 45°) and two "normal" washers with α of 3° and 10°. Micro-CT, a form of ICT, employs X-rays to obtain 2D cross-sections that can be stitched together to form a 3D rendering of the internal structure of an object. Figure 2E–G shows the micro-CT images with detected inclusions (purple) and pores (green) (see the Supporting Information for details). The washer with α = 3° was found to have ≈50 small pores distributed relatively symmetrically with some local concentration near the inner edge of the washer. The volume of these pores ranged from 1.1 to 5.2 × 10^{-4} mm^3; the volume of the washer is 198 mm^3. Molded Nylon 6 is known to be a slightly porous material.[3] The washer with α = 10° was observed to have ≈300 similarly sized pores concentrated symmetrically on the inner edge and asymmetrically on the outer edge of the washer. The washer that levitated with α = 45° was found to have an inclusion defect with a volume of 0.014 mm^3 (Figure 2G inset), significantly larger than the volume of the pores. The greater X-ray contrast of this region suggests that this defective region had a higher density than the surrounding Nylon 6.

DOI: 10.1002/adma.201405207

Notably, the MagLev technique was able to detect the presence of this defect in an opaque washer using a tabletop configuration of magnets in less than 10 s. In contrast, the micro-CT required ≈2 h per scan and several additional hours of computation and data analysis. Although micro-CT provides high-resolution information of the shape and location of the defect, such information may not be necessary for most quality control applications. Micro-CT, in addition, is only available in well-equipped facilities, requires skilled operators, costs several hundred thousand dollars, and is expensive to maintain. In a case where detailed structural information of a defect might not be necessary, MagLev could be used as an initial screening to save time and money. Here, MagLev can be used to infer that the inclusion defect in the washer was of higher density than the surrounding polymer because that region was closer to the bottom magnet. MagLev thus provides a simple, inexpensive means of determining the presence of inclusion defects in plastic parts.

We previously reported that an object of anisotropic shape, but homogeneous density, levitates in the device with its center of volume (centroid) located in the central axis of the MagLev device and orients so that it occupies the least amount of volume in regions of high magnetic field strength.[12] The controlling parameters are the lengths of the principal axes of the object, $\lambda_l \in (\lambda_u, \lambda_v, \lambda_w)$, which are geometric parameters that reflect how points within the object are distributed with regard to an arbitrary axis in the body-fixed frame of reference. For objects with regions of inhomogeneous density, for example, objects with defects, the effect of the distribution of mass on the orientation also has to be considered. To quantify the ability of the MagLev to identify defects, we extend this model here to also include the orientation of objects with an arbitrary distribution of density in MagLev. Equation 2 describes the potential energy U for an arbitrary object in a magnetic field, where $\Delta\chi = \overline{\chi}_s - \chi_m$, $\Delta\rho = \overline{\rho}_s - \rho_m$, $\mathbf{B} = \mathbf{B}(\mathbf{r})$ is the magnetic field, $\mathbf{r}_{cm} = (u_{cm}, v_{cm}, w_{cm})$ is the center of mass of the object (relative to its centroid) in the MagLev frame of reference, $\hat{z}$ is the unit vector of the z-axis, and V is the volume of the object. The primed coordinates indicate the frame of reference that is fixed with the orientation of the object (body-fixed frame of reference):

$$U = U_{mag} + U_{grav} = -\int_V \left(\frac{\Delta_\chi}{2\mu_o} \mathbf{B}\cdot\mathbf{B} + \Delta\rho g \mathbf{r}_{cm}\cdot\hat{\mathbf{z}} \right) dV \quad (2)$$

In general, for a diamagnetic object in a paramagnetic medium, $\Delta_\chi < 0$. Equation 3 gives the energy of orientation of the object in the MagLev (see the Supporting Information for full derivation and details). The second term in Equation 3 accounts for the gravitational torque on the object due to the asymmetric distribution of mass ($r_{cm} \neq 0$) within the object:

$$U(\theta,\phi) = -\frac{2B_0^2\Delta_\chi V}{\mu_o d^2}\left[\lambda_v^2 - \lambda_w^2 + (\lambda_u^2 - \lambda_v^2)\sin^2\phi\right] \sin^2\theta - \overline{\rho}_s V g (u_{cm}\sin\theta\sin\phi + v_{cm}\sin\theta\cos\phi + w_{cm}\cos\theta) \quad (3)$$

In this equation, we have assumed the magnetic field is linear $\left(\mathbf{B} = \frac{2B_o}{d} z\hat{\mathbf{z}}\right)$ and that Δ_χ is homogenous throughout the volume V of the object. Inspecting the first term (magnetic contribution), we see that, in general, the principal axes λ_l, which are determined by $\lambda_l^2 = \frac{1}{V}\int_V l^2\, dV$ for $l \in \{u, v, w\}$ (see the Supporting Information), will compete to determine the preferred orientation of the object in the magnetic field. For $r_{cm} = 0$, the second term in Equation 3 is zero and the largest λ_l will always orient perpendicular to the z-axis. If $r_{cm} \neq 0$, there will be an additional torque about the centroid that acts to tilt the object and move the center-of-mass downward. Just as the gravitational and magnetic forces balance at the equilibrium height of the object, the gravitational and magnetic torques balance at the equilibrium orientation—the equilibrium angle of orientation (θ,ϕ) will occur where U is minimized. We have ignored terms that depend on h because they do not couple to the angular orientation (Supporting Information).

We first consider the simple case of a rod with density ρ_r, length L, and square cross-section with side-length W. Because we are free to choose the starting orientation of the principal axes with respect to the MagLev reference frame, we chose a starting orientation of the rod such that the degenerate principal axes are $\lambda_u = \lambda_v$, and thus, for W along $\hat{\mathbf{u}}$ and $\hat{\mathbf{v}}$ and L along $\hat{\mathbf{w}}$, we have $\lambda_u^2 = \lambda_v^2 = W^2/12$ and $\lambda_w^2 = L^2/12$. If we now insert a small cubic inclusion with density ρ_i, volume V_i, and displacement w_i along the w-axis, then U simplifies to Equation 4:

$$U(\theta) = -\frac{B_0^2\Delta_\chi}{6\mu_o d^2} V(W^2 - L^2)\sin^2\theta + (\rho_i - \rho_r) V_i g w_i \cos\theta \quad (4)$$

The magnetic contribution (first term) to the equilibrium orientation of the rod is completely determined by the competition between W and L: i) for $L < W$ (short rod), the w-axis will orient toward $\theta_0 = 0°$ or 180° (L along z-axis) and ii) for $L > W$ (long rod), the w-axis will orient toward $\theta_0 = 90°$ or 270° (L along y-axis). In the first case, the gravitational torque is always zero when the inclusion is constrained to the w-axis. In the second case, if $V_i w_i \neq 0$, the final equilibrium angle will be $\theta = \theta_0 + \alpha$, where α is the angular deviation from magnetic equilibrium (θ_0), and is caused by a nonzero gravitational torque. In general, the side of the object with the defect will tip down if $\rho_i > \rho_r$ and will tip up if $\rho_i > \rho_r$. Larger values of V_i, $(\rho_i - \rho_r)$, or w_i will lead to larger values of θ. See Figure S1, Supporting Information, for examples. The rod-shaped geometry lends itself to relatively simple analytical treatment; more complicated geometries, and configuration of defects can be analyzed by numerically solving Equation 3.

To test our predictions experimentally, we used a 3D printer capable of printing materials with dissimilar densities to create model objects (see the Supporting Information for details). We made rods (L = 2.5 cm and W = 1.0 cm) out of polyacrylate (ρ_r = 1.184 g cm^{-3}) that incorporated a series of inclusions of the same material, but with a lesser degree of crosslinking and a lower density (ρ_i = 1.163 g cm^{-3}). The rods were fabricated with different inclusion volumes V_i and inclusion locations w_i (as measured from the centroid of the rod). Seven rods of each type were levitated in 0.05 M $MnCl_2$ in a MagLev device with rectangular prism magnets (2.5 × 2.5 × 10 cm, magnetized through the 2.5 × 10 cm face) used to confine the rods to the y-z plane (discussed in the Supporting Information) and α was recorded. We determined $B_0 = 0.385$ T with a magnetometer

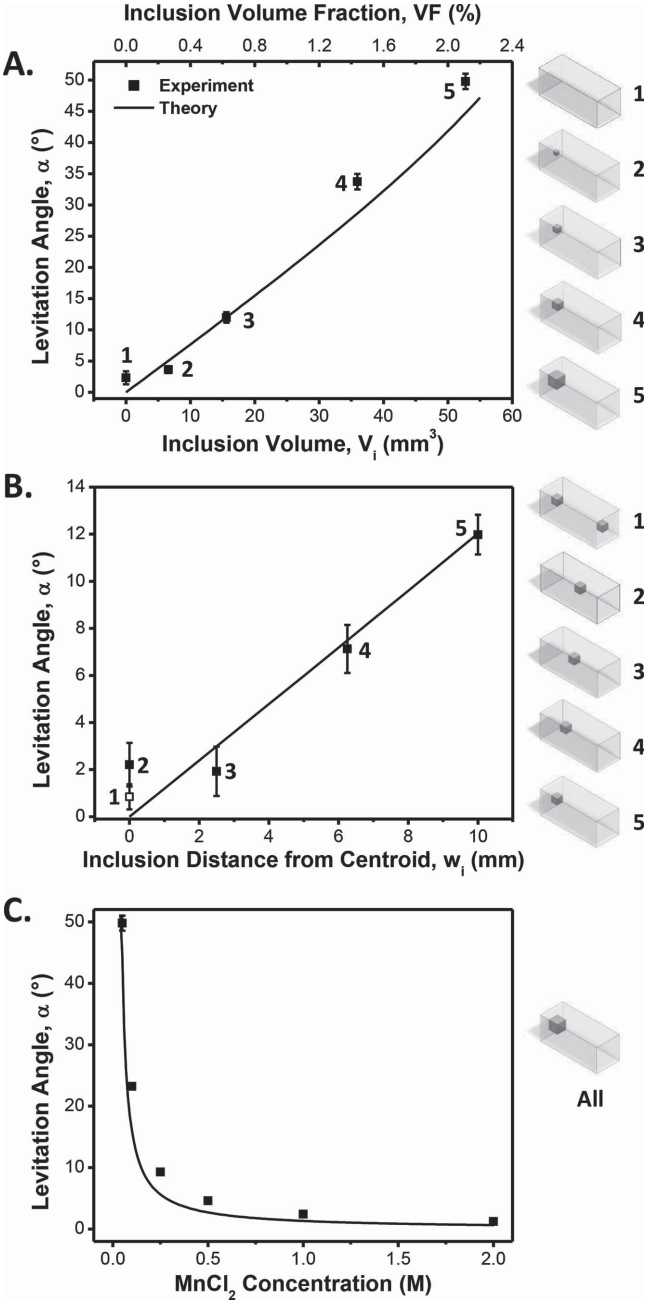

Figure 3. Levitation angle, α, for a variety of 3D-printed polyacrylate rods (ρ = 1.184 g cm^{-3}) containing inclusions of lower density polyacrylate (ρ = 1.163 g cm^{-3}) as a function of: A) inclusion volume, V_i, for a given location, w_i, B) inclusion distance from the centroid of the rod, and C) $MnCl_2$ concentration for a given inclusion size and location. Experimental data are shown as squares (n = 7), and results of calculations are shown as a solid line.

(AlphaLab, Inc.) and assumed $\overline{\chi}_s = 0.58 \times 10^{-5}$.[33] To determine χ_m at room temperature (296 K), we used the standard relation $\chi_m = 1.85811 \times 10^{-4}\left[\mathrm{Mncl}_2\right] - 9 \times 10^{-6}$, described by Mirica et al.[13]

Measurements (squares with error bars) and modeled values (solid line) are shown in **Figure 3**. As the V_i at a fixed w_i increases, from 6.6 to 52.7 mm^3, so does α (Figure 3A). Note that the pristine rod levitates at a small nonzero angle, most likely due to small non-uniformity in the crosslinking of polyacrylate. The volume fraction of an inclusion (VF), that is, the percentage of the total rod volume encompassed by the inclusion, is shown as an additional x-axis in Figure 3A. When the location is changed of an inclusion of a given volume (VF = 0.63%) is changed, α changes (Figure 3B); as the inclusion moves closer to the centroid of the rod, α decreased. Also shown (as an open square) is the levitation angle of a rod with two identical inclusions on opposing ends of the rod. One limitation of MagLev is that it is unable to detect a deviation from horizontal if the defects in an object are exactly symmetrical (or, in general, if additional defects do not shift the center of mass from the centroid), which is difficult to obtain except by design. If the difference in density due to the added inclusions was sufficiently large, however, the rods would levitate at a different height since the average density would be changed.

We quantified the sensitivity of MagLev as a method of detection for defects by selecting one type of rod/inclusion configuration (VF = 2.11%, w_i = 10 mm) and determining α for different concentrations of $MnCl_2$ (Figure 3C). As the concentration of the paramagnetic salt increased, α decreased. Thus, MagLev can be designed to detect defects within a certain tolerance by modifying the magnetic susceptibility of the medium.

We also used this analytical model to examine the effect on α of a single void (i.e., air pocket) of varying size in a 2.5-cm^3 rod. We found that, for a given MagLev setup (magnets = 2.5 × 2.5 × 10 cm, 4.5 cm apart), paramagnetic solution (0.05 M $MnCl_2$), and location of the void (w_i = 10 mm), even a small inclusion of 0.2 mm^3—only 0.008% of the total volume of the rod—would lead to a relatively large orientation angle ($\alpha > 10°$).

In addition to defects that arise during the manufacturing process, improper storage or use, or exposure to extreme environmental conditions, can lead to degradation of plastic parts that affects performance.[34] Plastics commonly undergo undesired changes in their properties upon exposure to a variety of environmental conditions (heat, moisture, UV-light, salt water, etc.).[3] Acids, salts, thermal stress, and UV-light are known to cause chain scissioning in polymers, including Nylon.[35] Currently, there is no simple method to detect degradation of parts due to exposure to damaging environmental conditions or improper storage. We hypothesized that chain scissioning and subsequent rearrangement of the polymer chains and migration of the scissioned monomers and oligomers through the polymer (or out into the environment) could lead to a decrease in density that can be detected using MagLev.

We simulated conditions of improper storage or use (excessive sun exposure) of Nylon 6/6 parts. We placed 30 rods, randomly oriented, in a container and exposed them to UV-light for 36 h (3.6 kW h). A control set of pristine rods was stored in the dark to simulate proper storage in a warehouse or toolbox. After the prescribed exposure period, each rod was rinsed with deionized (DI) water, placed into a solution of 0.10 M $MnCl_2$ + 1.26 M $ZnCl_2$ and levitated in a MagLev device. We measured α and plotted a histogram as shown in **Figure 4**. Pristine rods levitated with a clustered distribution of $\alpha < 3°$. The UV-light exposed rods, on the other hand, exhibited a large variation in α; the exposure caused a non-uniform change in density in many of the parts. In the container, some of the rods were

Adv. Mater. 2015,
DOI: 10.1002/adma.201405207

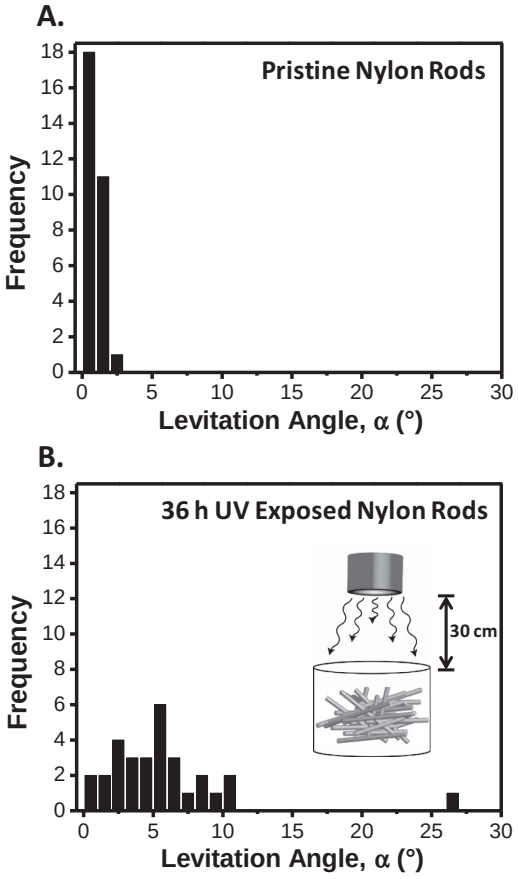

Figure 4. Histogram of the levitation angle, α, of A) pristine Nylon 6/6 rods or B) rods having been exposed to a 100 W UV-light for 36 h (3.6 kW h). For both cases, $N = 30$ rods and the paramagnetic solution was 0.075 M $MnCl_2$ in water.

entirely exposed to the UV light while others were only exposed over a small area due to the jumbled arrangement of the rods (see inset of Figure 4B).

To further understand these observations, we chose seven rods, exposed half of each rod to UV light (100 W), and measured the angle of the rods at 12-h intervals for 72 h. Figure S4, Supporting Information, shows α of the rods versus illumination time. The regions exposed to light show a reduction in density as evidenced by the positive α (measured as the exposed half above horizontal); we confirmed that the exposed region was responsible for the net decrease in density. The Supporting Information shows the behavior of rods subjected to other harsh environmental conditions, such as 50 °C deionized water, sea water (0.60 M NaCl), a solution of acid (0.10 M HCl), and localized thermal stresses (Figure S5 and S6, Supporting Information).

In addition to detecting defective parts, MagLev can be used to identify counterfeit parts that differ in density from genuine high-quality plastics. During the fabrication of high-value plastics, manufacturers (and counterfeiters) must control for molecular weight, crystallinity, porosity, and composition of additives.[36] Deviation from a controlled process for any of these parameters can alter the density of the material. Counterfeiting of high-value plastic parts is a serious challenge for the plastics industry and global trade regulators. In the absence of accepted industry standards or universal recognition of patent/branding rights, customers are forced to trust suppliers or rely on expensive and time-consuming testing methods to verify authenticity. For example, Tristar Plastics, the exclusive United States distributor of Rulon, a class of branded polytetrafluoroethylene (PTFE) derivatives, recommends seven characterization methods to ensure parts meet standards and are authentic: dynamic mechanical analysis, thermomechanical analysis, thermogravimetric analysis, differential scanning calorimetry, Fourier-transform infrared spectroscopy, scanning electron microscopy, and particle analysis.[36]

We obtained several types of real and fake Rulon from Tristar Plastics. Rulon bearings can cost several dollars per part (in comparison a Nylon washer which costs less than $0.10) and, in the case of Rulon 641, are United States Food and Drug Administration-approved for applications in the food industry, making them particularly attractive to counterfeiters. A search of the term "Rulon" on Alibaba.com, the world's largest online commerce site that hosts listings from independent manufactures and suppliers, reveals 82 suppliers with products claiming to be genuine Rulon. Fake Rulon is manufactured to closely match the color of genuine Rulon: fake and genuine Rulon 641 are visually indistinguishable.

We simultaneously levitated real and fake Rulon 641 in 0.40 M $MnCl_2$ in a 30% water, 70% Heavy Liquid (GEOLiquids, Inc.; 2.242 g cm^{-3}) solution and recorded the levitation height of each part. **Figure 5** shows a box plot of the levitation height of seven real and fake bearings and a representative image of the bearings levitating in a MagLev device. A significant difference (p-value = 2.8×10^{-6}) in average height between real and fake Rulon 641 was observed ($h_{avg} = 2.80 \pm 0.14$ and 1.24 ± 0.09 cm, corresponding to calculated $\rho_{avg} = 2.23 \pm 0.01$ and $\rho_{avg} = 2.27 \pm 0.01$). We also tested Rulon J, a derivative typically used for start-stop applications, and found that real and fake consistently levitate at different heights (Figure S7, Supporting Information). We also found that trace quantities of magnetic material in Rulon LR allowed us to use the detection of magnetic

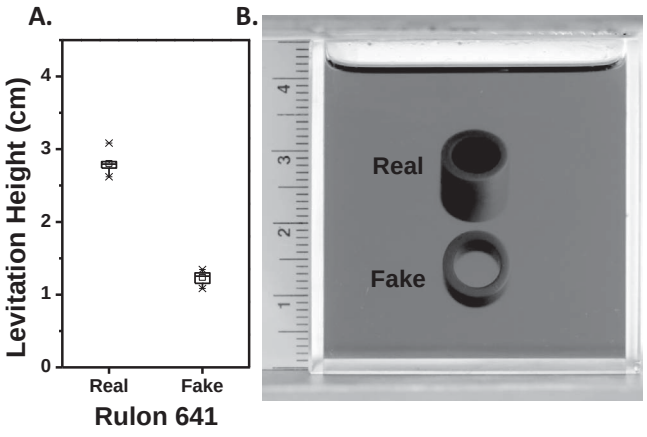

Figure 5. A) Box plot showing levitation height for real and fake Rulon 641 ($n = 7$) levitating at the same time. The significant difference in levitation height suggests a reproducible difference in density between real and fake Rulon. B) Photograph of representative real and fake Rulon 641 levitating in 0.40 M $MnCl_2$ in 30% water, 70% Heavy Liquid.

properties by MagLev as a further test of authenticity (see the Supporting Information for more details).

Taken together, these results suggest that MagLev can be used to detect defects in plastic parts by monitoring the levitation angle or height of the parts. Unlike flotation of a part in isodense salt brine (a state that is experimentally very difficult to achieve), MagLev does not require the density of the paramagnetic solution to match the density of the object perfectly. Furthermore, isodense flotation can only be used to determine whether an object is more dense or less dense than the carefully prepared solution; MagLev adds the benefits of: i) a magnetic restoring force that enables ordering of objects by density, and ii) a magnetic torque, caused by anisotropy in the shape of the object, that imposes a preferred alignment against which angular deviations can be compared.

The method is particularly useful for exposing defects in opaque parts where visual inspection is impossible. The orientation of a prototype part in MagLev can thus be used as a simple and rapid means to detect voids, crystalline regions, or inclusions during the manufacturing process. At the consumer end, MagLev can be used to detect the occasional defective part that may have skipped the quality control process. Furthermore, MagLev can detect the presence of regions of degraded polymer due to exposure to UV light and other harsh environments. In detecting counterfeit plastics, MagLev can save time and money at the point-of-sale by reducing the number of tests required to identify counterfeits (or increase the cost and complexity to counterfeiters by requiring density matching). If a batch of parts has a density significantly different than a verified authentic part, it can be assumed that the batch is not authentic and further testing is not necessary. We believe that along with plastic parts, measurement of heterogeneity in density using MagLev can be extended to detect defects in other materials, including fiber optic cables, ceramics, glass, and fire-protecting tiles, among others.

Supporting Information

Supporting Information is available from the Wiley Online Library or from the authors.

Acknowledgements

This work was funded by Bill and Melinda Gates Foundation Award No. 51308. D.Y. acknowledges the Wyss Institute for Biologically Inspired Engineering. A.K.E. acknowledges the Ford Foundation Postdoctoral Fellowship. The authors thank John Winzeler at Winzeler Gear and Dave Biering at TriStar Plastics for providing plastic parts, and for helpful discussions. The authors also thank Turgut Fettah Kosar for help with micro-CT analysis and James C. Weaver for help with 3D printing. This work was performed in part at the Center for Nanoscale Systems (CNS), a member of the National Nanotechnology Infrastructure Network (NNIN), which is supported by the National Science Foundation (NSF) under NSF Award No. ECS-0335765. CNS is part of Harvard University.

Received: November 13, 2014
Revised: December 18, 2014
Published online:

[1] *Handbook of Plastics Technologies*, (Ed: C. A. Harper), McGraw-Hill, New York **2006**.
[2] Z. Chen, L.-S. Turng, *Adv. Polym. Technol.* **2005**, *24*, 165.
[3] D. V. Rosato, D. V. Rosato, M. G. Rosato, *Injection Molding Handbook*, Kluwer, Dordrecht, The Netherlands **2000**.
[4] R. D. Adams, P. Cawley, *NDT Int.* **1988**, *21*, 208.
[5] V. Tvergaard, *Int. J. Fract.* **1982**, *18*, 237.
[6] R. M. McMeeking, *J. Mech. Phys. Solids* **1977**, *25*, 357.
[7] L. Xu, R. J. Crawford, *J. Mater. Sci.* **1993**, *28*, 2067.
[8] M. Bieberle, F. Barthel, H.-J. Menz, H.-G. Mayer, U. Hampel, *Appl. Phys. Lett.* **2011**, *98*, 34101.
[9] S. Persson, E. Östman, *Appl. Opt.* **1985**, *24*, 4095.
[10] Y. J. Song, W. Zhang, D. D. Wang, G. F. Jin, *Appl. Mech. Mater.* **2012**, *148*, 914.
[11] M. Kobayashi, *Int. J. Plast.* **1998**, *14*, 511.
[12] A. B. Subramaniam, D. Yang, H.-D. Yu, A. Nemiroski, S. Tricard, A. K. Ellerbee, S. Soh, G. M. Whitesides, *Proc. Natl. Acad. Sci. USA* **2014**, *111*, 12980.
[13] K. A. Mirica, S. S. Shevkoplyas, S. T. Phillips, M. Gupta, G. M. Whitesides, *J. Am. Chem. Soc.* **2009**, *131*, 10049.
[14] D. K. Bwambok, M. M. Thuo, M. B. J. Atkinson, K. A. Mirica, N. D. Shapiro, G. M. Whitesides, *Anal. Chem.* **2013**, *85*, 8442.
[15] M. R. Lockett, K. A. Mirica, C. R. Mace, R. D. Blackledge, G. M. Whitesides, *J. Forensic Sci.* **2013**, *58*, 40.
[16] N. D. Shapiro, K. A. Mirica, S. Soh, S. T. Phillips, O. Taran, C. R. Mace, S. S. Shevkoplyas, G. M. Whitesides, *J. Am. Chem. Soc.* **2012**, *134*, 5637.
[17] N. D. Shapiro, S. Soh, K. A. Mirica, G. M. Whitesides, *Anal. Chem.* **2012**, *84*, 6166.
[18] K. A. Mirica, S. T. Phillips, C. R. Mace, G. M. Whitesides, *J. Agric. Food Chem.* **2010**, *58*, 6565.
[19] M. B. J. Atkinson, D. K. Bwambok, J. Chen, P. D. Chopade, M. M. Thuo, C. R. Mace, K. A. Mirica, A. A. Kumar, A. S. Myerson, G. M. Whitesides, *Angew. Chem. Int. Ed.* **2013**, *52*, 10208.
[20] X. Yang, S. Y. Wong, D. K. Bwambok, M. B. J. Atkinson, X. Zhang, G. M. Whitesides, A. S. Myerson, *Chem. Commun.* **2014**, *50*, 7548.
[21] H. Pacheco-Martinez, L. Liao, R. Hill, M. Swift, R. Bowley, *Phys. Rev. Lett.* **2013**, *110*, 154501.
[22] K. A. Mirica, F. Ilievski, A. K. Ellerbee, S. S. Shevkoplyas, G. M. Whitesides, *Adv. Mater.* **2011**, *23*, 4134.
[23] T. Kimura, *Polym. J.* **2003**, *35*, 823.
[24] T. Kimura, S. Mamada, M. Yamato, *Chem. Lett.* **2000**, *29*, 1294.
[25] A. T. Catherall, P. López-Alcaraz, K. A. Benedict, P. J. King, L. Eaves, *New J. Phys.* **2005**, *7*, 118.
[26] R. D. Waldron, *Rev. Sci. Instrum.* **1966**, *37*, 29.
[27] I. Simon, *Rev. Sci. Instrum.* **1968**, *39*, 1666.
[28] R. Evrard, *J. Vac. Sci. Technol.* **1969**, *6*, 279.
[29] K. Guevorkian, J. M. Valles, *Proc. Natl. Acad. Sci. USA* **2006**, *103*, 13051.
[30] Y. Ikezoe, T. Kaihatsu, S. Sakae, H. Uetake, N. Hirota, K. Kitazawa, *Energy Convers. Manag.* **2002**, *43*, 417.
[31] Y. Ikezoe, N. Hirota, J. Nakagawa, K. Kitazawa, *Nature* **1998**, *393*, 749.
[32] N. Hirota, M. Kurashige, M. Iwasaka, M. Ikehata, H. Uetake, T. Takayama, H. Nakamura, Y. Ikezoe, S. Ueno, K. Kitazawa, *Physica B* **2004**, *346*, 267.
[33] Y. Ueda, F. Mishima, Y. Akiyama, S. Nishijima, *IEEE Trans. Appl. Supercond.* **2014**, *24*, 1.
[34] G. W. Ehrenstein, *Polymeric Materials: Structure, Properties, Applications*, Hanser Publications, Cincinnati, OH, USA **2001**.
[35] P. Thanki, C. Ramesh, R. Singh, *Polymer (Guildf)* **2001**, *42*, 535.
[36] Rulon Bearings: How to Recognize Genuine and Avoid Counterfeit, TriStar, Yorba Linda **2014**.